

XRF 050406 late time flattening: appearance of an IC component?

A. Corsi^{1,2,3} and L. Piro¹.

¹ IASF/INAF-Roma, Via Fosso del Cavaliere 100, 00133 Roma, Italy.

² Università degli studi di Roma “La Sapienza”, Piazzale Aldo Moro 5, 00185 Roma, Italy.

³ INFN - Sezione di Roma c/o Dip. di Fisica - Università degli studi di Roma “La Sapienza”, Piazzale Aldo Moro 5, 00185 Roma, Italy

ABSTRACT

Aims. We investigate on the possible evidence for Inverse Compton (IC) emission in the X-ray afterglow of XRF 050406.

Methods. In the framework of the standard fireball model, we show how the late time flattening observed in the X-ray light curve between $\sim 10^4$ s and $\sim 10^6$ s can be explained in a synchrotron plus IC scenario, when the IC peak frequency crosses the X-ray band.

Results. We thus conclude that the appearance of an IC component above the synchrotron one at late times successfully accounts for the X-ray observations.

Key words. gamma rays: bursts – X-rays: bursts – radiation mechanisms: non-thermal

1. Introduction

The “Burst Alert Telescope” (BAT; Barthelmy et al. 2005) on board Swift (Gherels et al. 2004) triggered GRB 050406 on 2005 April 6, at 15:58:48.40 UT (Parsons et al. 2005). BAT located the burst at RA=02^h17^m53^s and Dec=−50°10'52'' (J2000), with an uncertainty of 3 arcmin (Krimm et al. 2005). The photon index of the 15 – 350 keV time-averaged spectrum was $\Gamma = 2.38 \pm 0.34$ (Krimm et al. 2005). Due to the spectral softness, this burst was classified as an X-ray flash (XRF; Heise et al. 2001). The 15 – 350 keV fluence was $(1.0^{+1.13}_{-0.36}) \times 10^{-7}$ ergs cm^{−2} (Romano et al. 2006), which, at redshift of $z = 2.44$ (Schady et al. 2006), implies an isotropic energy release of $\sim 1.4 \times 10^{51}$ ergs.

The “X-Ray Telescope” (XRT; Burrows et al. 2005a) imaged the BAT field starting from 84 s after the trigger; the X-ray counterpart of XRF 050406 was found during the on-ground analysis (Cusumano et al. 2005; Capalbi et al. 2005). Also the “Ultra-Violet/Optical Telescope” (UVOT; Roming et al. 2005) started imaging about 88 s after the trigger. The optical afterglow was not detected on-board (Landsman et al. 2005), but subsequent on-ground analysis revealed a source within the XRT error circle (Rol et al. 2005). Late time observations (~ 7.8 hr after the burst) were performed by the Magellan/Clay Telescope, that found a single faint source ($R = 22.0 \pm 0.09$) located at RA=02^h17^m52^s.3 and Dec=−50°11'15'' (J2000; Berger et al. 2005a,b).

XRF 050406 X-ray light curve is particularly compelling: apart from the X-ray flare (Burrows et al. 2005b), it shows a

flattening at late times ($t > 4200$ s from the trigger). In this Letter we want to test if the flattening can be related with the appearance of an IC component, in the context of the standard fireball model (Sari et al. 1998). In Sect. 2 we collect the available afterglow information. We refer to the 0.2 – 10 keV light curve and spectral analysis by Romano et al. (2006); to Table 1 in Schady et al. (2006) for the optical data. In Sect. 3 we constrain the parameters of the fireball in a synchrotron plus IC scenario and in Sect. 4 we give our conclusions.

Hereafter, $F(\nu, t) \propto t^{-\alpha} \nu^{-\beta}$; $E_{52} = E/(10^{52}$ ergs), n is in units of 1 particle/cm³, $\epsilon_{B,-2} = \epsilon_B/10^{-2}$, $\epsilon_{e,0.5} = \epsilon_e/0.5$; p is the power-law index of the electron energy distribution; $z = 2.44$ is the adopted redshift (Schady et al. 2006).

2. The optical-to-X-ray afterglow

The 0.2 – 10 keV light curve of XRF 050406 shows a complex behavior (Burrows et al. 2005b), with a power-law decay underlying a flare peaking at about 210 s after the trigger and a flattening between $\sim 10^4$ s and $\sim 10^6$ s. Romano et al. (2006) found that, excluding the flare, a broken power-law model with $\alpha_1 = 1.58^{+0.18}_{-0.16}$, $\alpha_2 = 0.50 \pm 0.14$ and $t_{\text{break}} \sim 4200$ s yields a good fit to the data.

Using an absorbed power-law with the Hydrogen column density (N_{H}) fixed to the Galactic value of 2.8×10^{20} cm^{−2} (Dickey & Lockman 1990), a mean X-ray photon index of $\Gamma = 2.1 \pm 0.3$ ($\beta = 1.1 \pm 0.3$) during the first 600 s after the trigger and $\Gamma = 2.06 \pm 0.24$ ($\beta = 1.06 \pm 0.24$) between ~ 600 s and $\sim 2 \times 10^4$ s, was found (Romano et al. 2006). The 3σ upper-limit for the total (Galactic plus intrinsic) N_{H} along the line of sight is of 9×10^{20} cm^{−2} (Romano et al. 2006).

The first UVOT observations were performed in the V -band, between 113 s and 138 s. The highest measured flux was in a 50 s exposure 113 s after the trigger, where the measured magnitude was 18.92 ± 0.31 (Schady et al. 2006). Correcting for Galactic extinction with $E(B-V) = 0.022$ mag and $A_V/E(B-V) = 3.1$ (Schlegel et al. 1998), this implies a V -band flux of 0.11 ± 0.04 mJy. At about 100 s, using a conversion factor of 6.5×10^{-11} erg cm $^{-2}$ count $^{-1}$ and a spectral index of $\beta \sim 1.1$ as found by Romano et al. (2006), the 0.2 keV flux was of ~ 0.05 mJy. The observed optical-to-X-ray spectral index is thus $\beta_{opt-X} \sim 0.15$ at ~ 100 s, extremely flat. We note that such a flat value was not found in the analysis performed by Schady et al. (2006), where the mean optical and X-ray fluxes between 220 s and 950 s were used.

3. Synchrotron plus IC model

Chincarini et al. (2005) and Nousek et al. (2005) have underlined that Swift GRB X-ray light curves usually present an initial steep decay (until ~ 500 s) followed by a shallower one; around a few thousands seconds later, further steepening is observed. In the case of XRF 050406, the initial slope is shallower than usual, $3 \leq \alpha \leq 5$ (Tagliaferri et al. 2005), and the curvature relation $\alpha = \beta + 2$ is not satisfied. This suggests that the emission preceding the late time flattening could be part of the afterglow (Romano et al. 2006) rather than the tail of the prompt. In this scenario, the superimposed flare could be interpreted as a late internal shock (Burrows et al. 2005b; Romano et al. 2006); on the other hand, if the flare marks the onset of the afterglow (Piro et al. 2005; Galli & Piro 2006), the analysis here presented is valid for $t > 210$ s.

In this section we want to test if a model in which the steep part of the X-ray light curve is related to standard synchrotron emission while the late time flattening to the appearance of an IC component, agrees with the data.

3.1. Synchrotron component

To constrain the synchrotron component, we summarize in Table 1 the closure relationships between the spectral index β and the early temporal decay index α_1 for the X-ray afterglow.

$$\nu_m = 2 \times 10^{13} \frac{f(p)}{f(2.5)} (1+z)^{1/2} \epsilon_{B,-2}^{1/2} \epsilon_{e,0.5}^2 E_{52}^{1/2} t_d^{-3/2} \text{ Hz} \quad (1)$$

is the injection frequency, where $f(p) = \left(\frac{p-2}{p-1}\right)^2$, and

$$\nu_c = 2.7 \times 10^{15} (1+z)^{-1/2} \epsilon_{B,-2}^{-3/2} E_{52}^{-1/2} n^{-1} t_d^{-1/2} (1+x)^{-2} \text{ Hz} \quad (2)$$

is the cooling frequency (Sari & Esin 2001); t_d is the observer's time in units of days; x is the ratio of the inverse Compton to synchrotron luminosity, i.e. $\sim \sqrt{\epsilon_e/\epsilon_B}$ in the fast cooling regime and $\sim \sqrt{\epsilon_e/\epsilon_B} \times (t/t_{IC}^0)^{-(p-2)/(2(4-p))}$ in the slow cooling IC-dominated regime (Sari & Esin 2001); t_{IC}^0 is the time at which the transition from slow cooling to fast cooling takes place (when ν_m equals ν_c). It is important to note that if IC is an efficient cooling mechanism, the transition to slow cooling is delayed by a factor of ϵ_e/ϵ_B (Sari & Esin 2001), i.e. until times

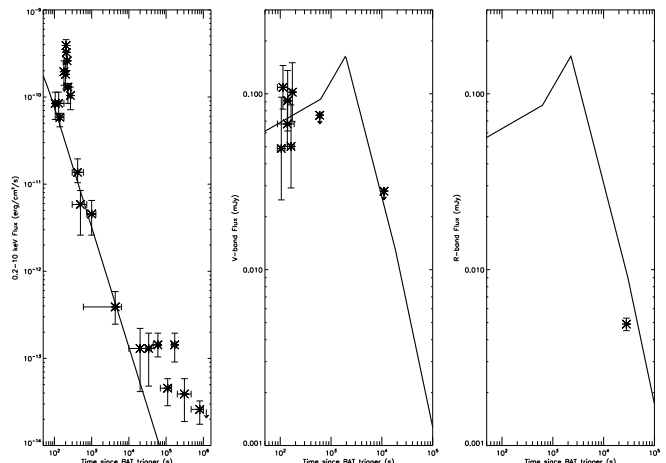


Fig. 1. 0.2 – 10 keV (left panel), V -band (central panel) and R -band (right panel) light curves in a standard synchrotron fireball model where $\epsilon_B = 0.19$, $\epsilon_e = 6.3 \times 10^{-2}$, $E_{52} = 0.5$, $n = 0.1$, $p = 2.5$, so to fit the optical and X-ray fluxes at 100 s, i.e. to satisfy the conditions $\nu_m(100 \text{ s}) \sim 0.2 \text{ keV}$, $\nu_c(100 \text{ s}) \sim 0.03 \text{ keV}$ (see text).

when it is usually assumed to be already in the slow cooling phase.

On the basis of the closure relationships, scenarios b), c) and d) are compatible with the observations in both an ISM and a Wind environment (Chevalier & Li 1999). Hereafter, we will limit our discussion to an ISM. In case b), one gets $\langle p \rangle = 2.5 \pm 0.3$. In case c), $\langle p \rangle = 3.1 \pm 0.3$. In case d), if we just consider synchrotron emission, the same relation of case b) holds. The addition of IC modifies the expression of ν_c for a factor $(1+x)^{-2}$; as a consequence, the temporal decay index is modified from its synchrotron only value of $3/4(p-1) + 1/4$ to $3/4(p-1) + 1/4 - (p-2)/(8-2p)$ (Sari & Esin 2001; Corsi et al. 2005) and the corresponding closure relationship is the one indicated in parenthesis in Table 1.

We have seen in Sect. 2 that the optical-to-X-ray spectral index before the flare is rather flat. In a standard synchrotron scenario, this can be explained by the synchrotron peak frequency being between the optical and the X-ray band. If $\nu_m(100 \text{ s}) \sim 0.2 \text{ keV}$ and $\nu_c(100 \text{ s}) \sim 0.03 \text{ keV}$, one gets the lowest peak flux required to fit the optical and X-ray data around 100 s. However, under these conditions, the injection frequency crosses the V -band around 2×10^3 s; until that time, the light curve (Fig. 1) features a rise. In the case of XRF 050406, at ~ 600 s the source was no longer visible above the background (Schady et al. 2006), thus suggesting a progressive fading of the optical afterglow. We note that the V -band upper-limits adopted here are standard 3σ upper-limits, so the corresponding limiting flux is 3 times higher than the value reported by Schady et al. (2006), where the upper-limits were given as the error on the net counts.

To account simultaneously for a flat optical-to-X-ray spectrum, a fast decreasing X-ray light curve and a *decreasing* optical emission, while *overestimating as less as possible* the optical flux around ~ 100 s, it is convenient to set $\nu_m(100 \text{ s}) \sim 0.2 \text{ keV}$ and $\nu_c(100 \text{ s}) \leq 5.45 \times 10^{14} \text{ Hz}$. In this case, the op-

Table 1. Closure relationships between the spectral and temporal indices of the X-ray afterglow ($\beta = 1.1 \pm 0.3$, $\alpha_1 = 1.58 \pm 0.17$) in the standard synchrotron fireball model for a Wind or ISM environment. In parenthesis are the relationships in an ISM modified for the effect of IC cooling; (u) means that IC emission does not modify the closure relationship with respect to its synchrotron-only value.

| ISM environment | | Wind environment | | | |
|-----------------|-------------------------|--|-------------------------------------|----------------------------|-----------------|
| | Expected relation | Observed value | Expected relation | Observed value | |
| a) | $\nu_c < \nu_X < \nu_m$ | $2\alpha - \beta = 0$ (u) | 2.1 ± 0.4 | $2\alpha + \beta - 1 = 0$ | 3.3 ± 0.5 |
| b) | $\nu_c < \nu_m < \nu_X$ | $2\alpha - 3\beta + 1 = 0$ (u) | 0.86 ± 0.96 | $2\alpha - 3\beta + 1 = 0$ | 0.86 ± 0.96 |
| c) | $\nu_m < \nu_X < \nu_c$ | $2\alpha - 3\beta = 0$ (u) | -0.14 ± 0.96 | $2\alpha - 3\beta - 1 = 0$ | -1.1 ± 1.0 |
| d) | $\nu_m < \nu_c < \nu_X$ | $2\alpha - 3\beta + 1 = 0$ ($\alpha + \frac{3\beta^2 - 6\beta + 1}{2(2-\beta)} = 0$) | 0.86 ± 0.96 (0.48 ± 0.31) | $2\alpha - 3\beta + 1 = 0$ | 0.86 ± 0.96 |

tical light curve does not feature any rise. The optical-to-X-ray spectral index does not depend on p and has a value of 0.5, which is the flattest as possible in a standard synchrotron scenario if the peak frequency is below the optical band (and $p > 2$). Normalizing to the X-ray emission around 100 s, the predicted V -band flux is however overestimated of a factor of ~ 5 . Requiring additional extinction in the GRB host galaxy or a contribution to the early X-ray flux coming from the rising part of the flare (or a combination of these two effects) helps accounting for the early broad-band observations, as we will see in the following section.

3.2. IC component

We now consider the possibility of explaining the flattening observed in the late part of the afterglow as the appearance of an IC component. Following the prescriptions given by Sari & Esin (2001), the IC component is modeled assuming a power-law shape similar to the synchrotron one, plus logarithmic corrections if important in the considered regime. In the power-law only approximation, the IC spectrum is normalized to a peak flux value of $f_{max}^{IC} = 2 \times 10^{-7} f_{max} n (R/10^{18})$, where f_{max} is the peak flux of the synchrotron component and R is the fireball radius in cm (Sari & Esin 2001).

In Fig. 2 we show how for a reasonable choice of parameters, $\epsilon_B = 1.9 \times 10^{-4}$, $\epsilon_e = 0.25$, $E_{52} = 5$, $n = 100$, the late time flattening in the X-ray light curve can be explained with the passage of ν_m^{IC} in the X-ray band. As expected (Sect. 3.1), if no local extinction is added, the predicted R - and V -band fluxes are overestimated of a factor of ~ 5 and ~ 2.4 , respectively. In a “Small Magellanic Clouds” (SMC)-like environment (Pei 1992), at $z = 2.44$, $A(V_{int}) \sim 0.32$ mag allows to recover consistency with the optical data (Fig. 3, solid lines); this implies an absorption of $N_H \sim 0.32 \times 1.6 \times 10^{22} \text{ cm}^{-2}$. In such an environment, due to the lower metallicity, the upper-limit of $9 \times 10^{20} \text{ cm}^{-2}$ set by the XRT analysis should be increased of a factor of ~ 7 (Stratta et al. 2004) and thus the required N_H should be compared with this increased limit.

If before the X-ray flare there is some contribution from the rising part of the flare itself (as one may expect in a late internal shock scenario), we can relax to some extent the normalization condition. In Fig. 4 we show a possible solution, with $\epsilon_B = 9.0 \times 10^{-4}$, $\epsilon_e = 0.36$, $E_{52} = 1$, $n = 350$ (that give $\nu_m(100 \text{ s}) \sim 0.6 \text{ keV}$). In this case the logarithmic corrections to the IC spectrum are important between 0.2–10 keV, and have

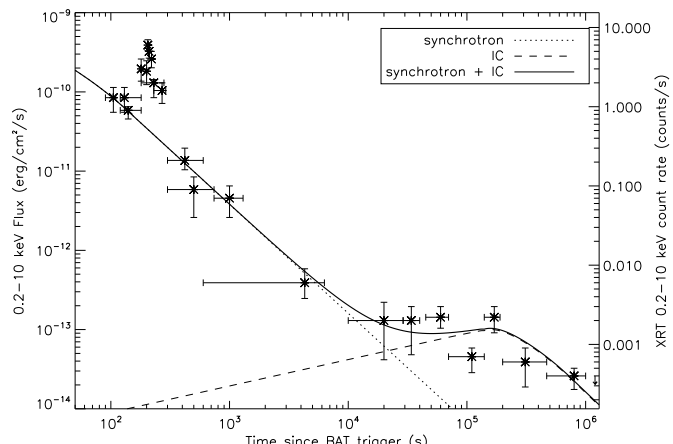


Fig. 2. Synchrotron plus IC model predictions for the 0.2–10 keV light curve with $\epsilon_B = 1.9 \times 10^{-4}$, $\epsilon_e = 0.25$, $E_{52} = 5$, $n = 100$, $p = 2.5$.

been added to the power-law approximation. The IC peak flux has been normalized to a value of $f_{max}^{IC} = 14/45 \times f_{max} \sigma_T n R$ (Sari & Esin 2001), where σ_T is the Thompson cross section.

In the optical band (Fig. 3, dashed lines), adding a Galactic-like extinction (Cardelli et al. 1989, with $R_V = 3.1$) of $A(V_{int}) \sim 0.15$ mag locally to the GRB site, explains both the R - and V -band observations. A similar solution can be found in a SMC-like environment with $A(V_{int}) \sim 0.13$ mag (Fig. 3, dotted lines). The implied local N_H are $\sim 0.15 \times 1.79 \times 10^{21} \text{ cm}^{-2}$ and $\sim 1.6 \times 0.13 \times 10^{22} \text{ cm}^{-2}$ respectively, both fully compatible with the upper-limit from the X-ray analysis (what noted before should be kept in mind when considering the N_H value in the SMC case).

From a spectral point of view, since in this scenario the flattening is associated with the passage of the IC peak frequency in the X-ray band, in that portion of the light curve a spectral index varying between $-1/3$ and $\sim (p-1)/2$ (or between $-1/3$ and $p/2$ plus logarithmic term correction for the solution with some contribution from the flare) is expected. For XRF 050406, due to the dimness of the source, we have no info on the spectral index after 2×10^4 s; future observations will thus be of key importance to confirm or reject the scenario we are suggesting.

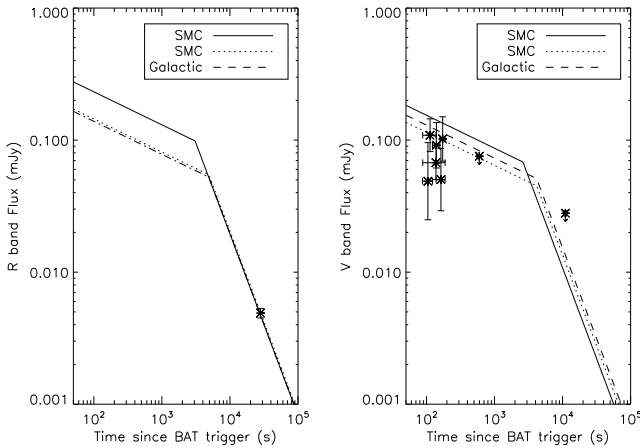


Fig. 3. Synchrotron plus IC model predictions in the R - (left panel) and V -band (right panel). The fireball parameters are as in Fig. 2 for the solid lines and as in Fig. 4 for the dotted and dashed ones. Solid lines include a SMC-like local ($z = 2.44$) extinction of $A(V_{int}) \sim 0.32$ mag; dotted lines a SMC-like $A(V_{int}) \sim 0.13$ mag; dashed lines a Galactic-like $A(V_{int}) \sim 0.15$ mag.

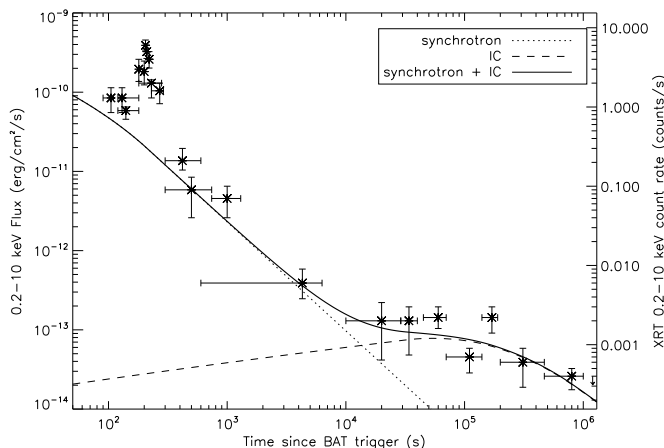


Fig. 4. Synchrotron plus IC model predictions for the $0.2 - 10$ keV light curve with $\epsilon_B = 9 \times 10^{-4}$, $\epsilon_e = 0.36$, $E_{52} = 1$, $n = 350$, $p = 2.5$.

4. Conclusions

We discussed XRF 05406 afterglow in the context of the standard fireball model. Within a synchrotron plus IC scenario, we tested if the late time flattening observed in the X-ray light curve can be explained with the appearance of an IC component. We found that setting $\epsilon_B = 1.9 \times 10^{-4}$, $\epsilon_e = 0.25$, $E_{52} = 5$, $n = 100$, the X-ray observations can be well explained. Considering also the optical data, we noted that the early optical-to-X-ray spectral index appears rather flat and requires additional extinction to recover marginal consistency with the data. We also proposed a second solution, with $\epsilon_B = 9 \times 10^{-4}$, $\epsilon_e = 0.36$, $E_{52} = 1$, $n = 350$, where the optical-to-X-ray normalization problem is solved requiring that at $t < 210$ s

some contribution to the X-ray emission comes from the rising part of the flare. Using a Galactic- or SMC-like extinction curve, the N_H required by the optical data is consistent with the upper-limit found in the X-ray analysis.

Acknowledgements. L. Piro acknowledges support of the EU through the EU FPC5 RTN “Gamma-ray burst, an enigma and a tool”; A. Corsi acknowledges the support of an INFN grant. A. Corsi thanks G. Montani and P. Schady for useful discussions.

References

- Barthelmy, S. D., Barbier, L. M., Cummings, J. R., et al. 2005, *Space Sci. Rev.*, 120, 143
- Berger, E., Kulkarni, S. R., Fox, D. B., et al. 2005a, *ApJ*, 634, 501
- Berger, E., Oemler, G., & Gladders, M. 2005b, *GRB Coordinates Network*, 3185
- Burrows, D. N., Hill, J. E., Nousek, J. A., et al. 2005a, *Space Sci. Rev.*, 120, 165
- Burrows, D. N., Romano, P., Falcone, A., et al. 2005b, *Science*, 309, 1833
- Capalbi, M., Perri, M., Romano, P., et al. 2005, *GRB Coordinates Network*, 3184
- Cardelli, A., Clayton, G. C., & Mathis, J. S. 1989, *ApJ*, 345, 245
- Chevalier, R. A. & Li, Z.-Y. 1999, *ApJ*, 520, L29
- Chincarini, G., Moretti, A., Romano, P., et al. 2005, *ApJ*, submitted to, astro-ph/0506453
- Corsi, A., Piro, L., Kuulkers, E., et al. 2005, *A&A*, 438, 829
- Cusumano, G., Kennea, J., Burrows, D. N., et al. 2005, *GRB Coordinates Network*, 3181
- Dickey, J. M. & Lockman, F. J. 1990, *ARA&A*, 28, 215
- Galli, A. & Piro, L. 2006, to appear in *A&A*
- Gherels, N., Chincarini, G., Giommi, P., et al. 2004, *ApJ*, 611, 1005
- Heise, J., in't Zand, J., Kippen, R. M., & Woods, P. M. 2001, *Gamma-Ray Bursts in the Afterglow Era*, 16
- Krimm, H., Barbier, L., Barthelmy, S., et al. 2005, *GRB Coordinates Network*, 3183
- Landsman, W., Hunsberger, S., Breeveld, A., et al. 2005, *GRB Coordinates Network*, 3182
- Nousek, J. A., Kouveliotou, C., Grupe, D., et al. 2005, *ApJ*, submitted to, astro-ph/0508332
- Parsons, A., Barthelmy, S., Cummings, J., et al. 2005, *GRB Coordinates Network*, 3180
- Pei, Y. C. 1992, *ApJ*, 395, 130
- Piro, L., De Pasquale, M., Sofitta, P., et al. 2005, *ApJ*, 623, 314
- Rol, E., Schady, P., Hunsberger, S., et al. 2005, *GRB Coordinates Network*, 3186
- Romano, P., Moretti, A., Banat, P. L., et al. 2006, to appear in *ApJ*, astro-ph/0601173
- Roming, P. W. A., Kennedy, T. E., Mason, K. O., et al. 2005, *Space Sci. Rev.*, 120, 95
- Sari, R. & Esin, A. A. 2001, *ApJ*, 548, 787
- Sari, R., Piran, T., & Narayan, R. 1998, *ApJ*, 497, L17
- Schady, P., Mason, K. O., Osborne, J. P., et al. 2006, to appear in *ApJ*, astro-ph/0601182

Schlegel, D. J., Finkbeiner, D. P., & Davis, M. 1998, ApJ, 500,
525

Stratta, G., Fiore, F., Antonelli, L. A., et al. 2004, ApJ, 608,
846

Tagliaferri, G., Goad, M. R., Chincarini, G., et al. 2005, Nature,
436, 985